



## Adsorption Equilibrium, Kinetics and Thermodynamic Studies of Aqueous Phase Abatement of Basic dyes Using Clay Interpolated with Cationic Surfactant

<sup>1\*</sup>Chigbundu C. Emmanuel, <sup>2</sup>Kayode O. Adebawale and <sup>2</sup>Bamidele I. Olu-owolabi

<sup>1</sup>Chemical and Food Sciences Department, Bells University of Technology, Ota, Ogun State, Nigeria

<sup>2</sup>Department of Chemistry, Faculty of Sciences, University of Ibadan, Ibadan, Nigeria

\*Correspondence Email: [ecchigbundu@bellsuniversity.edu.ng](mailto:ecchigbundu@bellsuniversity.edu.ng)

### ABSTRACT

The adsorptive uptake of two synthetic dyes – Saffranin-O (Basic Red (BR2)) and Methylene Green (Basic Green (BG5)) from aqueous solution at different adsorbent dose, pH, adsorbent-adsorbate contact time and temperature by hexadecyltrimethyl ammonium bromide (CTAB) intercalated kaolinite (CTIK) clay has been studied and compared with native raw kaolinite (NRK) clay. NRK and CTIK were characterized using different analytical techniques including pH at point of zero charge (pzc), bulk density, methylene blue adsorption (MBA) surface area, scanning electron microscopy (SEM) coupled with Energy dispersive X-ray (EDX), Fourier transform infrared spectroscopy (FTIR) and X-ray Diffraction (XRD). The FT-IR and XRD analyses results for CTIK compared to NRK revealed, respectively, that Amide I and II, hydroxyl, and carbonyl functional groups on CTIK surface are involved in characteristic active sites for adsorption and the reflections at  $2\theta$  degree =  $5.79^\circ$  calculated using Bragg's formula showed interlayer space expansion ( $\Delta d$ ) equivalent to 8.028 Å. The experimental data were fitted with the Freundlich, Langmuir, and Sips's isotherm models for adsorption equilibrium determination whereas pseudo-first order, pseudo-second order and Elovich equation were employed for adsorption kinetic studies. To validate the accuracy of models' prediction, several error statistical goodness-of-fit criteria were applied. Using nonlinear regression curve, the adsorption kinetics is best interpreted with the Elovich model ( $R^2 > 0.98$ ) for the basic dyes adsorption onto both adsorbents followed by the pseudo-second-order model ( $R^2 > 0.97$ ). The best fit isotherm model followed the order; Sips ( $R^2 > 0.99$ ) > Langmuir ( $R^2 > 0.96$ ) > Freundlich ( $R^2 > 0.89$ ). Model applicability tests revealed an irreversible adsorptive reaction and chemisorption based on kinetic and isotherm models, respectively. The thermodynamic parameters revealed that the adsorption process was spontaneous and endothermic in nature. CTIK was more effective for basic dye uptake than NRK and had a higher affinity for BG5 than BR2 dye.

**Keywords:** Adsorption, Basic Dyes, Cationic Surfactant, Equilibrium, Intercalation, Kinetic

### INTRODUCTION

Manufacturing firms have indiscriminately discharged wastewater and industrial effluents including dyes and other harmful organic pollutants into water bodies. This is due to a lack of commitment on the side of government officials in charge of monitoring and regulation of waste management (Omole and Isiorho, 2011; Yaseen and Scholz, 2016). The presence of these pollutants in freshwater resources has rendered it unfit for human consumption, constituting a health and environmental hazard. This natural resource is becoming increasingly unavailable, and its scarcity is causing huge social and economic concerns (Omole and Isiorho, 2011). As a result, the challenge of protecting freshwater bodies has become a key concern of research in recent years in order to ensure a healthy human population while also protecting the aquatic environment (Omole and Isiorho, 2011).

To a considerable extent, the pursuit of technological advancement and industrialization is responsible for environmental contamination, particularly where lakes and rivers have been overburdened with toxic compounds after being used as a limitless dumping ground for waste disposal (Kushwaha, 2015). When it comes to industrialization, dye houses take the lead because of their potential to provide a wide range of work possibilities and their global and local integration with many economic sectors (Yaseen and Scholz, 2019).

Dye industry is an important part in textile, pharmaceutical paper and pulp, printing, cosmetic and other chemical industries. Dyes are recalcitrant organic, colored, synthetic toxicants in water that are complex in nature, not easily biodegraded and are stable to light irradiation (Imran *et al.*, 2015). They obstruct sunlight light penetration into water hence hinders the photosynthetic activities of aquatic plant (Hassan

and Carr, 2018). They cause series of ailments such as cancer, allergy, eye and skin irritation (Aquino *et al.*, 2014; Khatri *et al.*, 2018). For the treatment of dye-bearing wastewater, several physical, chemical, and biological procedures such as adsorption, biosorption, ozonation, coagulation/flocculation, advanced oxidation, membrane filtering, and liquid-liquid extraction have been widely used (Ashtekar *et al.*, 2013; Bruno *et al.*, 2019). Adsorption is a highly effective separation process that is presently considered to be preferable to other water treatment procedures in terms of initial cost, ease of design, and insensitivity to harmful compounds (Rashed, 2011; Jadhav and Jadhav, 2021).

Basic dyes such as Saffranin O (BR2) and Methylene green (BG5) are highly water-soluble dyes. They are cationic dyes used as a laboratory aid in testing. BR2 is a derivative of Pyrazine while BG5 is thiazine derived. These dyes have been studied for their potential to irritate the skin, eyes, and gastrointestinal tract. It has the potential to influence blood variables like clotting, as well as cause somnolence and respiratory difficulties. They are employed as dyes, tranquilizers, and insecticides, among other things. For example, BG5 could indeed convert ferric iron in hemoglobin to ferrous iron, resulting in red blood cell disintegration. Therefore, an increased interest has been focused on removing of these dyes from the wastewater (Adebowale *et al.*, 2014, Chigbundu and Adebowale, 2021).

Clay minerals used as inorganic adsorbents for adsorption namely, montmorillonite-(smectic group), kaolinite, Illite, bentonite and chlorite have been reported as the main classes of clay minerals by Adeyemo *et al.*, (2017). As many scientists and research studies have demonstrated, these inorganic adsorbents are layered, small particle sized, hydrous and aluminosilicates (Adebowale *et al.*, 2014; Kodama and Grim 2014; Adeyemo *et al.*, 2017). Their high adsorption and cation exchange capacity is the result of effectiveness in the adsorption of pollutants from aqueous effluents (Chaari *et al.*, 2015; Adeyemo *et al.*, 2017).

Natural clay materials have hydrophilic properties and are not particularly viable for the uptake of organic pollutants which are hydrophobic in nature (Akyuz *et al.*, 1993; Bennani-Karim *et al.*, 2011). As a result, these clay minerals have been discovered to absorb organic contaminants from water exceptionally well when their surfaces are modified with organic modifiers, resulting in their hydrophobicity (Rahmat *et al.*, 2020). Researchers in the field of water treatment have recently focused their efforts on modifying clay with organic compounds (also referred as organoclay) that could improve its adsorption or hydrophobic qualities for adsorbing organic pollutants (Han *et al.*, 2019; Munir *et al.*, 2019). By this productive insight, organoclays are therefore

used to replace costly and toxic adsorbents in wastewater treatment because of their low cost, great natural availability, relatively remarkable specific surface area, outstanding adsorption capacity, non-toxic nature, and ease of modification (Nafees and Waseem 2014; Anirudhan and Ramachandran, 2015). For example, in a particular work Bentonite was modified with cationic surfactant (Hexadecyltrimethyl ammonium chloride)/organoclay for the adsorption of methylene blue (MB), Crystal violet (CV) and Rhodamine B (RB) from simulated wastewater (Nafees and Waseem 2014; Anirudhan and Ramachandran 2015). In another research work, organophilic organoclay modification of smectite was obtained by the intercalation of long-chain quaternary ammonium ions of the general form  $[(CH_3)_3NR]^+$  or  $[(CH_3)_2NR]^+$ , where R is the alkyl hydrocarbon for reducing the leachability of pentachlorophenol (PCP) (Perelomov *et al.*, 2021). With this consideration, locally sourced kaolinite clay sample was modified to organoclays by using hexadecyltrimethyl ammonium bromide (CTAB) as modifier in this work.

## MATERIALS AND METHODS

### Materials

Pristine natural raw kaolinite clay was collected from behind the levees of the Niger delta, Aniocha south Delta state, Nigeria. Basic Red 2 (BR2) and Basic Green 5 (BG5) dyes were supplied by BDH Prolabs chemicals. Cethyltrimethylammonium Bromide (CTAB) was supplied by Sigma Aldrich. All the reagents used were analytical grade and were used without further purification.

### Methods

#### Preparation of intercalated adsorbent

The pristine natural raw kaolinite clay (NRK) was purified and the organic matter present was oxidized by treatment with peroxide solution (Austin *et al.*, 2018; Adebowale *et al.*, 2014). Adopting and modifying the procedure used by Martín *et al.*, (2018), 20.0 g of the purified NRK was dispersed in 500 mL of 0.25 M NaCl solution (approximately equivalent to 15.00 g/1000 cm<sup>3</sup>) and agitated continuously for several hours to exchange any replaceable metal ion on the kaolinite clay with sodium ion. The recovered solid was then washed free of chloride with distilled de-ionized water (tested with AgNO<sub>3</sub> solution). The product, which is sodium-exchanged NRK was dried at 333 K and gently ground to powder. 10.0 g of the Na-exchanged NRK was dispersed in the solution of 400.0 mL distilled de-ionized water containing 5.0 g of CTAB. The mixture was placed in a flat-bottom flask fitted with a condenser, heated at 353 K and agitated on a hot plate with magnetic stirrer for 10 h each day. The intermittently monitored accumulated timing was 100 h (10 days). The sample was properly rinsed with distilled de-

ionized water before being dried in an oven at 333 K. The CTAB intercalated kaolinite (CTIK) was softly ground into powdery particles and sieved to a particle size < 350 µm after drying.

### Batch adsorption experiment

Stock solutions of the dyes were prepared by dissolving 1.0 g of each of the dyes in a litre of distilled de-ionized water. An aliquot concentration of the dyes necessary for the experiment were then prepared from the stock by serial dilution with distilled de-ionized water using mathematical expression in Equation 1.

$$C_2 = \frac{V_1 \times C_1}{V_2} \quad (1)$$

Where  $V_1$  and  $V_2$  are Volumes of adsorbate dye solution taken from the stock and volume prepared by dilution respectively (L), while  $C_1$  and  $C_2$  are the concentration of the stock and concentration required (mg/L), respectively.

The Adsorption Experiments were conducted in completely mixed batch reactors by employing bottle-point technique for each data point (Pei-Yee and Zaini, 2020; Isiuku *et al.*, 2019). This was accomplished by placing 0.8 g of adsorbent in a sequence of bottles, adding 300 mL of a solution of 200 mg/mL concentration of the adsorbate to each, and tumbling all bottles for long time enough to guarantee sorption equilibrium. After an equilibration interval, the reactors and their contents were centrifuged to separate solid and solution phase concentrations and solid-phase concentrations of the adsorbed sorbate were estimated by difference. Effect of various operating conditions on adsorption (such as pH variation, adsorbent dose variation, dye concentration variation (for adsorption equilibrium study), contact time (for adsorption kinetic study) and temperature variation (for thermodynamic study) were investigated using this method. The quantities of the unadsorbed dye after each adsorption process were calculated using the wavelength of BR2 or BG5 dyes which was determined using UV-vis spectrophotometer (Surgifriend SM7504UV/visible 911) to be at  $\lambda_{max} = 520$  or 663 nm respectively. The dyes' adsorption capacity in weight per weight

and in percentage was determined using the formula of equations 2 and 3.

$$Q_e = \frac{(C_o - C_e) \times V}{m} \quad (2)$$

$$\% = \frac{(C_o - C_e) \times 100}{C_o} \quad (3)$$

Where  $Q_e$  is the quantity adsorbed per unit gram (mg/g),  $C_o$  and  $C_e$  are the initial and equilibrium dye concentrations (mg/L) while  $V$  is the volume (L) and  $m$  is the mass (g).

### Physicochemical characterization

Surface features of both NRK and CTIK adsorbent samples were described instrumentally with SHIMADZU Fourier Transform Infrared (FTIR) spectrometer using KBr to identify the functional groups. Scanning Electron Microscope (SEM) Quata200 Model, USA for surface morphology and PHILIPS PW3040/60 X'Pert X-Ray Diffractometer (XRD) for crystallographic changes. Some of the physicochemical characteristics of the adsorbents investigated were their Bulk densities (BD) ( $\text{g/cm}^3$ ) using the method employed by Blistan *et al.* (2020), Point of zero charges (PZC) by Nwosu *et al.* (2018), Surface area (SA) ( $\text{m}^2/\text{g}$ ) determination using Methylene Blue Adsorption (MBA) method by Skripkina *et al.* (2020) and Cation exchange capacity (CEC) (meq/100 g) by the method adopted by Yousefi *et al.* (2018).

### Adsorption Isotherms and Kinetic studies

By fitting a suitable adsorption isotherm model to the experimental data, the relationship between quantity adsorbed and quantity remaining in the bulk in solution at equilibrium during the adsorption process was studied. Using nonlinear regression curves, different isotherm model equations (Table 1) were considered to predict the behaviours of the basic dyes toward the adsorbent.

The kinetic evaluation on adsorption experimental data, a nonlinear form of regression curve was used to provide information about optimum conditions, adsorption pathway, and likely rate controlling step prediction. The kinetic model equations are shown in Table 1.

**Table 1: Mathematical expression of non-linear Isotherm and Kinetic model equations**

Models	Non-linear Equation	Parameter	Plot	Ref
<b>Isotherm Model</b>				
Langmuir,	$q_e = \frac{q_m K_L C_e}{1 + K_L C_e}$	qm, K <sub>L</sub>	qe vs Ce	Overah, 2020
Freundlich,	$q_e = K_F C_e^{1/n}$	K <sub>F</sub> , n	qe vs Ce	Overah, 2020
Sips	$q_e = \frac{q_s a_s C_e^{1/n_s}}{1 + a_s C_e^{1/n_s}}$	qs, as, ns	qe vs Ce	López-Luna <i>et al.</i> , 2019
<b>Kinetic Model</b>				
PFO*	$q_t = (q_e - \exp^{-K_1 t})$	qe, K <sub>1</sub>	qt vs t	López-Luna <i>et al.</i> , 2019
PSO*	$q_t = \frac{K_2 q_e^2 t}{1 + K_2 q_e t}$	qe, K <sub>2</sub>	qt vs t	Boparai <i>et al.</i> , 2011
Elovich	$q_t = \frac{1}{\beta} \ln(1 + \alpha \beta t)$	α, β	qt vs t	López-Luna <i>et al.</i> , 2019

\*Key: PFO is Pseudo-First Order; PSO is Pseudo-Second Order; k<sub>1</sub> represents the rate constant for pseudo-first order adsorption; k<sub>2</sub> represents the overall rate constant for pseudo-second order adsorption (g/mg min); K<sub>L</sub> is Langmuir constant related to adsorption capacity (mg g<sup>-1</sup>); q<sub>m</sub> the maximum amount of adsorbate adsorbed at equilibrium (mg/g); K<sub>F</sub> is related to adsorption capacity (L/mg); 1/n is the heterogeneity factor; a<sub>s</sub> is Sips isotherm model constant (Lg<sup>-1</sup>); n<sub>s</sub> is Sips isotherm exponent (Lg<sup>-1</sup>); β represents the initial adsorption Elovich rate (mg/g min), while α is the extent of surface coverage (g/mg)

### Thermodynamic parameter study

Thermodynamic parametric including enthalpy (ΔH°), entropy (ΔS°), and Gibbs free energy (ΔG°) of adsorption. By the use of determined Langmuir adsorption isotherm constant, K<sub>L</sub> (Equation 4) and the van't Hoff equation thermodynamic parameters of the adsorbents were evaluated alongside conventional thermodynamic equations 5 - 7 (Obayomi *et al.*, 2020).

$$K_L = \frac{q_e}{C_e} \quad (4)$$

$$\Delta G^\circ = -RT \ln K_L \quad (5)$$

Where K<sub>L</sub> is the Langmuir isotherm constant, R (8.315 JK<sup>-1</sup>mol<sup>-1</sup>) is the gas constant and T (K) is the operating temperature.

$$\Delta G^\circ = \Delta H^\circ - T\Delta S^\circ \quad (6)$$

Therefore the van't Hoff equation becomes:

$$\ln K_L = \frac{-\Delta H^\circ}{RT} - \frac{\Delta S^\circ}{R} \quad (7)$$

The value of standard enthalpy change (ΔH°) and standard entropy change (ΔS°) for the adsorption process are thus determined from the slope and intercept of the plot of lnK<sub>L</sub> vs. 1/T (equation 7).

### Error analysis

The error analysis was used to further affirm the goodness of fit of the Isotherm and kinetic models. These includes the highest value of Coefficient of determination (R<sup>2</sup>) and lowest value of Root Mean Square Error (RMSE), Marquardt's percent standard deviation (MPSD), Average relative error (ARE), Sum of the absolute errors (EABS), Chi-square analysis (χ<sup>2</sup>), Standard error (SE) and sum of the squares of the errors (ERRSQ).

## RESULTS AND DISCUSSION

### Physicochemical characteristics of the adsorbent

The bulk density (BD) of a solid sample is usually investigated in order to determine the compactness and weight per total volume occupied by sorbent materials like NRK and CTIK. The BD test measures the flow uniformity and solid sample packaging quantity, both of which have a significant impact on adsorbate uptake. Generally, higher density adsorbent holds more adsorbate per unit volume (Adegoke *et al.*, 2017). From Table 2 the bulk density of CTIK is in the range of 1.33 to 1.21 g/cm<sup>3</sup>, higher than that of NRK adsorbent which is in the range of 1.15 to 0.97 g/cm<sup>3</sup>. The higher value of BD is an indication of higher compactness in nature of CTIK because of its crystal formation as a result of intercalation. Similar value was obtained in the literature by Nwosu *et al.* (2018), who reported a value of 1.42 g/cm<sup>3</sup> for unmodified kaolinite which is within the range of the value of the unmodified kaolinite (NRK) in this work (Table 2).

Specific surface area (SSA) was also investigated to measure the adsorbent's surface area and micropore volume which are the key factors in determining whether the material is suitable for the removal of pollutants from aqueous solution. The specific surface area, which includes the total sum of all pore volume, is believed to have contributed to the adsorbent's ability to accommodate adsorbate. The SSA of NRK and CTIK adsorbents as shown in Table 2 were determined using methylene blue adsorption method and the values obtained were in the range between 23.97 - 23.95 and 33.03 - 32.69  $\text{m}^2 \text{g}^{-1}$  were respectively. Different results were obtained in the literature by researchers for example by Vdović *et al.*, (2010) (SSA = 39  $\text{m}^2/\text{g}$ ) and Macías-Quiroga *et al.* (2018), (SSA = 45  $\text{ml}^2/\text{g}$ ) for kaolinite. This could be due to differences in SSA determination methodologies and adsorbent sampling sources.

The point of zero charge (PZC) or the border line between positivity and negativity of charges on the surface of an adsorbent can be determined by a single pH value of an adsorbent.

The PZC of NRK and CTIK were determined and found to be  $5.18 \pm 0.014$  and  $4.95 \pm 0.021$  respectively (Table 2). In research works in literature, Boukhemkhem and Rida, (2017) reported a value of PZC = 3.1 for unmodified kaolinite, Appel *et al.* (2003) recorded a range of PZC value of 2.7 – 3.2 while the value reported by Mahmood *et al.* (2011) was 5.6. From these results it is obvious that the PZC values for unmodified kaolinite are not the same and did not even agree with our result of PZC value of 5.18. According to Mahmood and coworkers, PZC results are often inconsistent, and no sample has a stable PZC value.

As per the modified adsorbent (CTIK), the functionality on the surface influence and determine the value of the adsorbent samples's pH at the PZC. According to Ibrahim *et al.* (2019), when the pH of an adsorbent is greater than the PZC, the number of positively charged sites on the adsorbent decreases while the number of negatively charged sites increases, and vice versa. Hence CTIK with the least PZC at around pH = 4.95 will possess an increased negatively charged sites at pH > 4.95 (Table 2).

**Table 2: Physicochemical Characterisation of Adsorbents**

Parameters	NRK	CTIK
BD ( $\text{g}/\text{cm}^3$ )	$1.06 \pm 0.09$	$1.27 \pm 0.06$
PZC	$5.18 \pm 0.014$	$4.95 \pm 0.021$
SSA ( $\text{m}^2\text{g}^{-1}$ )	$23.97 \pm 0.02$	$33.03 \pm 0.34$

### Adsorbent characterization

Figure 1 showed the scanning electron micrographs of NRK, CTIK and their elemental composition via energy dispersive x-ray spectroscopy (EDXS). NRK micrographs (Fig. 1 (a) and (b)) revealed that the adsorbent sample is made up of grainy tiny particles that are of few micrometers in size and also observable is the sponge-like shape typical of kaolinites (Mbaye *et al.*, 2014). Mbaye *et al.* (2014) reported a similar finding, explaining that the platelet-like particles found were layered at random on top of each other. The visual representation of the elemental composition of the NRK sample obtained by EDXS analysis is shown in Figure 1c. This information from the EDXS firstly confirmed the existence of alumina, silica, and oxygen as the main mineral compositions supporting the aluminosilicate chemical nature of kaolinite clay (Fig. 1 (c) and (f)). Additionally, are many other counter ions including iron, which is linked to its brownish

colouration. Meanwhile, the micrographs of CTIK images, as shown in figures 1 (d) and (e), revealed that their particles are bigger, with uninterruptedly rough surfaces that appeared flake-like in texture, tightly bounded together by intermolecular forces. Interestingly, the surface of CTIK appeared whitish, indicating the presence of organic modifiers that affected the small particles of untreated clay minerals (Sun *et al.*, 2017). The spectrogram and elemental composition of the CTIK obtained from EDXS are shown in Figure 1f, still retained higher percentages of Al, Si, and O elemental composition in addition to Carbon, Bromine, and Nitrogen, which are as a result of the modifier's inclusion (CTAB). On the EDXS of NRK (Fig. 1c), the disappearance of various ions (such as Fe, Ti) that were present in lesser proportions was noticed. The possibility of bonding between the active sites on the mineral and ions of the organic modifier, due to the presence of N could explain this observation (Fig. 1f).

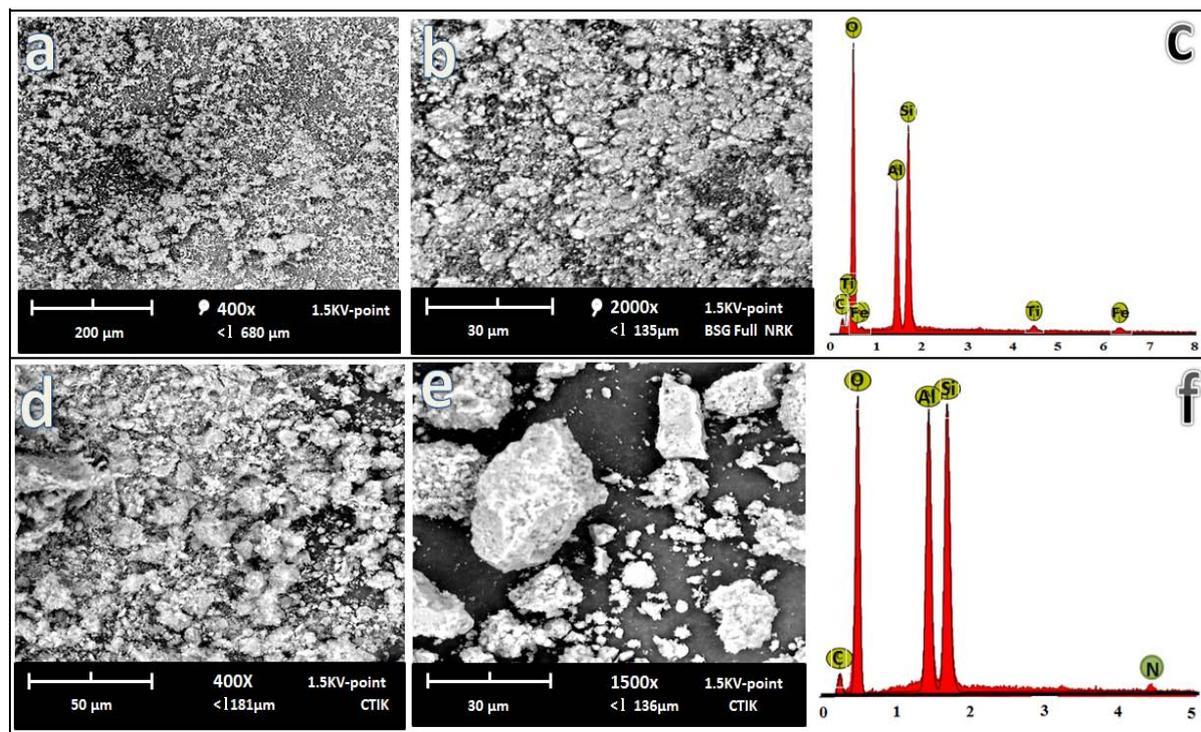


**Figure 1: Scanning Electron Micrographs (SEM) of (a) NRK clay particles (x400) (b) NRK clay particles (x2000) (d) CTIK modified clay (x400) and (e) CTIK modified clay (x1500). While SEM-Energy Dispersive X-Ray analysis of (c) NRK clay particles and (f) CTIK modified clay. Fourier transform infrared spectroscopy (FTIR)**

The FTIR spectroscopy spectra graph for NRK and CTIK are compared as shown in Figure 2. The regions of the graph with notable specific vibration bands common to kaolinite were broken off (not displayed). These corresponds to Si–O stretching vibration at  $1109$  and  $1040$   $\text{cm}^{-1}$ , Si–O bending vibration at  $469$   $\text{cm}^{-1}$  and Si–O–Si group of the tetrahedral sheet at  $1031$   $\text{cm}^{-1}$ . The other bands at  $913$   $\text{cm}^{-1}$  and  $526$   $\text{cm}^{-1}$  were assigned to Al–OH and Si–O–Al deformation which are typical of kaolinite clay mineral. These peaks were in good agreement with those reported in the literature by Saikia and Parthasarathy, (2010); Meziane *et al.* (2017); Aldhayan and Aouissi(2017); Mustapha *et al.* (2019). The O–H vibration of the inner hydroxyl surface (interlamellar) was assigned to the peaks at  $3695$   $\text{cm}^{-1}$ ,  $3665$   $\text{cm}^{-1}$ , and  $3652$   $\text{cm}^{-1}$  on both NRK and CTIK graphs, whereas the band at  $3620$   $\text{cm}^{-1}$  was due to the O–H vibration of inner hydroxyl groups (intralamellar).

According to the literature, the mobility of the band reported at  $3620$   $\text{cm}^{-1}$  lacked spontaneity, which is characteristic of the stretching of the inner OH groups in the kaolinite framework, due to the chemical interaction between the silica and alumina

sheets. Interlayer adjustments usually have little effect on this particular internal OH- group, and it does not contribute in the formation of hydrogen bonds with the intercalated molecules (Meziane *et al.* 2017). The absorption bands on NRK observed at  $3437$   $\text{cm}^{-1}$  and  $3317$   $\text{cm}^{-1}$  were attributed to the OH of water molecules. On both graphs, at  $1631$   $\text{cm}^{-1}$ , another absorption band corresponding to water deformation was observed (not shown) (Bakhtary *et al.*, 2013; Asuha *et al.*, 2015)

The bands at  $2924$  and  $2852$   $\text{cm}^{-1}$  observed on the graph of CTIK were assigned to the stretching vibration methyl ( $\text{CH}_3$ ) and methylene ( $\text{CH}_2$ ) groups. Besides, the  $\text{CH}_3\text{-N}$  of CTAB molecule was found on CTIK's graph to have a widened and weaker absorption bands for secondary amines at  $3248 - 3014$   $\text{cm}^{-1}$ . Zenasni *et al.* (2014), also reported this as a single peak at  $3014$   $\text{cm}^{-1}$ . Another discovered peaks are around  $1650$   $\text{cm}^{-1}$  and  $1600$   $\text{cm}^{-1}$ (very low intensity) was assigned to carbonyl ( $\text{C=O}$ ) and -N–H groups that are related with amide I and amide II, respectively. Mincke *et al.*, (2019) also reported values of  $1649$  and  $1572$   $\text{cm}^{-1}$  for the amide I ( $\text{C=O}$ ) and amide II (N–H) bonds, respectively, which were closer to the wave numbers observed in this study.

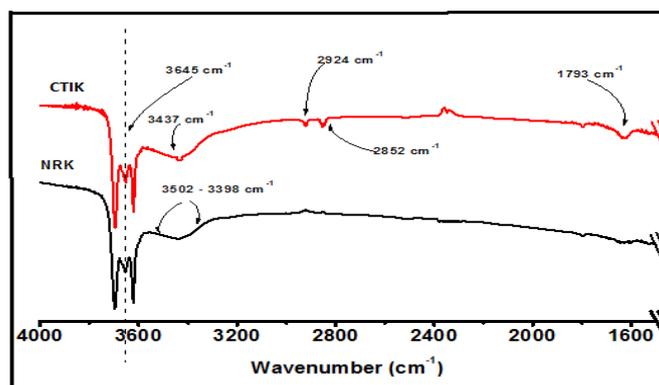


Figure 2: FTIR Spectra for NRK and CTIK

### X-ray diffraction (XRD) study

The XRD diffractogram patterns of both NRK and CTIK adsorbent samples are shown in figure 3. At  $2\theta$  degree =  $12.35^\circ$ , NRK graph showed a peak intensity equivalent to basal reflection (d-spacing) of =  $7.17 \text{ \AA}$  ( $0.725 \text{ nm}$ ) characteristic peak according to Maged *et al.* (2020). These findings are in good agreement with the similar observation that was previously reported (Zuo *et al.*, 2017). The XRD pattern shown on the diffractograms of CTIK adsorbent

(Fig. 3) when compared with that of NRK, revealed that (apart from kaolinite clay characteristic peak) there were additional new peaks on the intercalated adsorbent's diffractogram observed in Figure 3. These additional sharp peaks are reflections at  $2\theta$  degree =  $5.79^\circ$  for CTIK equivalent to basal reflection (d-spacing) of  $15.197 \text{ \AA}$  (equivalent to  $1.52 \text{ nm}$ ). The calculation of interlayer space expansion ( $\Delta d$ ) using Bragg's formula  $d = 8.028 \text{ \AA}$  which can be attributed to the presence of CTAB molecule in the interlayer space of the clay.

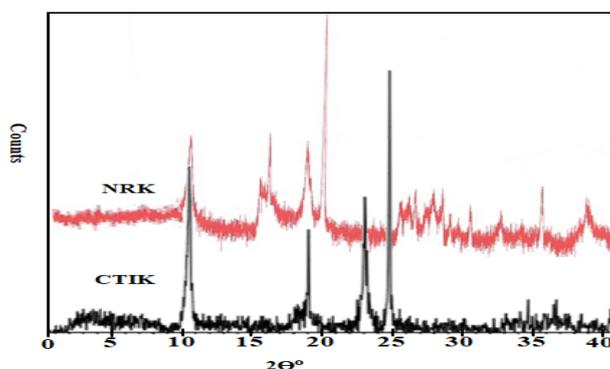


Figure 3: X-ray diffraction (XRD) pattern of NRK and CTIK adsorbent samples

### ADSORPTION STUDY

#### Effect of pH

One of the most important effective characteristics that can affect the strong affinity between adsorbent and adsorbate is the pH of the solution. The study of the impact of pH on the adsorptive uptake of basic dyes by the adsorbents helps in revealing the adsorption capacity of the adsorbent and the efficiency of the process. According to Rápó and Tonk, (2021), the chemistry of adsorbate in solution, competition with coexisting ions in the solution, the activity of functional groups on the adsorbent surfaces, and their surface charges are all affected by pH. The pH of the solution can influence not just the adsorbent but also the chemical structure of the dye. This is shown in Figure 4. The figure showed that the percentage dye removal increases as the pH

increases. These are most likely the outcome of the NRK and CTIK adsorbents' capacity to achieve surfaces with the ability to interact with BR2 and BG5 dyes adsorbate via ion exchange, electrostatic forces, or even the creation of inner sphere complexes in solution at high pH or in alkaline environment (Šljivić-Ivanović and Smičiklas, (2020). However the interaction between the adsorbent and the adsorbate points to the direction of being by more of electrostatic force. This is because the pH at point zero charge (pHpzc) for both NRK and CTIK are at pH = 5.18 and 4.95 respectively (Table 2). According to Zakaria *et al.* (2017) as the pH of a solution rises above PZC, the surface of the adsorbent becomes negatively charged, attracting the positively charged adsorbate to the adsorbent via electrostatic attraction.

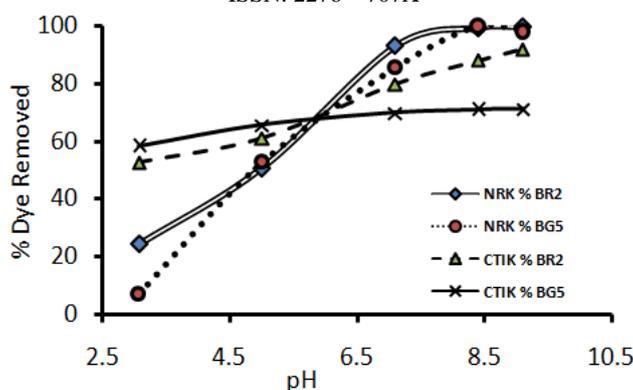


Figure 4: Effect of pH on the percentage of basic dye removed by NRK and CTIK

#### Effect of adsorbent dose variation

The effect of varying the adsorbent dosage on the adsorption process was investigated by keeping the adsorbate concentration constant while changing the adsorbent dose in grams at each experimental run. As shown in Figure 5, the quantity of cationic (BR2 and BG5) dyes uptake reduces as the mass of NRK and CTIK adsorbents increases. This can be described as follows: as the amount of adsorbent in grams increases, so does

the total number of adsorption active sites in the presence of the same adsorbate concentration, resulting in inverse proportionality in adsorption. Similar results have been reported by other authors (Padmavathy *et al.*, 2016; Nwosu *et al.*, 2018). When NRK and CTIK uptake capacity for BG5 is compared to BR2 dye uptake capacity, it is clear that NRK and CTIK uptake capacity for BG5 is higher.

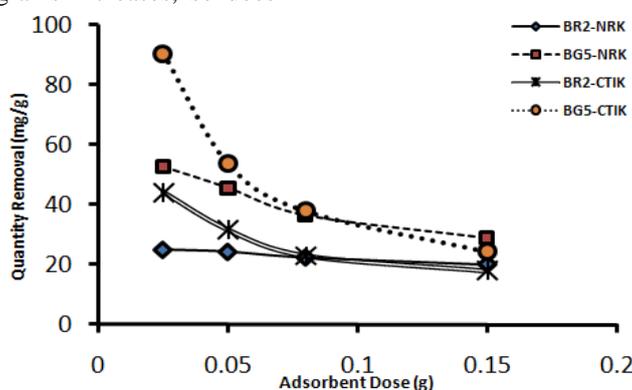


Figure 5: Adsorbent dose variation

#### Adsorption equilibrium study

Equilibrium Adsorption Studies allow for the collection and analysis of numerical data on an adsorbent's quantitative capabilities. It also establishes a link between the amounts of adsorbate uptake onto an adsorbent surface at a specific temperature. The empirical values were (graphically) fitted to Freundlich, Langmuir, and Sips isotherm models using non-linear isotherm regression curves. The implementation of the nonlinear optimization strategy, which currently acts as an alternative to obtaining the isotherm parameter values, has been facilitated by advances in computational technology (Moussout *et al.*, 2018; Charles 2019; Valdivia *et al.*, 2021). It was further supported by the results of goodness of fit obtained from least value of error analysis using statistical error formula, in addition to the coefficient of determination ( $R^2$ ) that was used as a criterion for selecting the best fitted isotherm models for dye adsorption, as shown in table 3. The fitting of isotherm models to experimental data for

the adsorption of BR2 and BG5 dyes onto NRK and CTIK adsorbents (graph not shown) revealed a sharp rise in curve. This indicates that a considerable quantity of initial dyes were adsorbed at low concentrations (between 0 and 10 mg/L), after which the quantity adsorbed began to gradually decline as the concentration increased, indicating that the process is approaching equilibrium. As the dye concentration increased, the slope remained nearly constant, indicating that the adsorbent surface adsorption sites were saturated.

For the adsorption of both basic dyes (BR2 and BG5) onto NRK and CTIK, equilibrium isotherm studies revealed that the Sips isotherm produced better fits (from the values of correlation coefficients,  $R^2$  and the least error values presented in Table 3). It's worth noting that the Langmuir isotherm was only the second best of the better fitted models for the adsorption of both dyes by NRK and CTIK, with Freundlich isotherm coming in third. This simply implies that the NRK and

CTIK surfaces are mostly homogeneous in nature, with only a few heterogeneous binding sites. In other words, when the BR2 and BG5 dyes were bonded to the adsorbent surfaces, a monomolecular layer formation was observed. Therefore, using Sips model as the criteria for the adsorbents (that is NRK and CTIK) adsorption capacities

determination for the uptake of BR2 and BG5 dyes, CTIK is 15 – 20 mg/g and 30 - 35 mg/g for BR2 and BG5, respectively and NRK is 15 – 20 mg/g and 20 - 25 mg/g for BR2 and BG5, respectively (Table 3). Evidently, modification has shown to influence adsorption capacity of NRK as presented by CTIK adsorbent.

**Table 3: Adsorption Isotherm model and their parameters for different adsorbents**

Isotherm Model	Parameter	NRK		CTIK	
		BR2	BG5	BR2	BG5
<b>Langmuir</b>					
	$Q_{max}$ (mg/g)	14.41	21.33	13.06	26.39
	$K_L$ (L/mg)	58.92	44.94	5.41	7.49
	$R^2$	0.89	0.96	0.89	0.96
	ERRSQ	38.64	28.59	29.39	44.77
	MPSD	111.47	81.07	103.43	113.77
	ARE	88.74	46.94	34.29	38.56
	EABS	0.81	-1.32	10.47	15.31
<b>Freundlich</b>					
	$K_F$ (L/mg)	6.97	10.08	6.43	10.56
	$n_F$	0.14	0.14	0.13	0.16
	$R^2$	0.87	0.88	0.93	0.95
	ERRSQ	47.66	92.48	19.88	58.27
	MPSD	193.73	236.87	114.61	169.48
	ARE	268.1	400.62	47.58	65.19
	EABS	0.98	2.51	12.48	18.98
<b>Sips</b>					
	$Q_{ms}$ (mg/g)	15.69	21.79	17.09	31.97
	$K_s$ (L/mg)	0.51	1.88	0.75	0.16
	$n_s$	0.38	0.75	0.36	0.42
	$R^2$	0.90	0.97	0.98	0.99
	ERRSQ	35.58	28.64	6.25	16.18
	MPSD	141.87	83.37	59.69	67.21
	ARE	143.77	49.65	22.91	21.44
	EABS	0.86	-0.09	5.18	9.3

## ADSORPTION KINETIC STUDIES

### Contact time

Contact time is used to determine the optimum time for adsorbate – adsorbent interaction in an adsorption process. The effect of contact time on the adsorption of BR2 and BG5 basic dyes onto NRK and CTIK adsorbents was investigated, with the results shown graphically in Figure 6. The adsorption of the basic dyes increased to a large extent for both adsorbents when the contact time was increased up to 195 min., and then remained somewhat constant after that. This could be attributed to the initially abundance of free unoccupied binding sites on the adsorbents' surfaces, followed by a much slower phase when the active sites become saturated as the system approaches equilibrium. Adeyi *et al.* (2019) reported a similar curve in their study on the adsorption of cationic dye onto Thiourea-Modified Polymer. It was therefore considered that the system reached equilibrium shortly after the inflection point above 200 minutes.

### Kinetics study

The non linear forms of pseudo-first-order and pseudo-second-order kinetic models, as well as the Elovich equation, were used to analyze the adsorption kinetic data obtained from the study of the effect of contact time in order to determine the speed of adsorption and the fundamental mechanisms of adsorbent-adsorbate interaction. The highest value of coefficient of determination ( $R^2$ ) and the lowest value of error analysis parameters (namely Chi-square test ( $\chi^2$ ), Standard error (SE), and Root mean square error (RMSE)) are the criteria chosen for selecting the appropriate model that can best explain the rate and mechanism of kinetics of the adsorption process (Table 4). The curves of these kinetic models after nonlinear fitting are shown in Figure 7, and the values of the kinetic parameters obtained are shown in Table 4. Meanwhile Table 1.contains the equations that define these kinetic models.

As can be observed, the Elovich model was the best fit when  $R^2$  criterion is being utilized for best fit model selection. According to Adeyi *et al.* (2019) the widely held belief that models with larger  $R^2$  accurately reflect the researched events is

not enough. They argued that fitting data with any of the non-linear equations based solely on coefficient of determination functions is insufficient proof or a requirement for the description of a mechanism that controls the kinetics or dynamics of adsorption in a specific system. Despite the fact that they are frequently used as a foundation for evaluating the quality of kinetic model fitting to experimental data in the literature, doing error analysis to show the certainty of the observed fitting is necessary to further prove the fitted model's assumption. Elovich had the smallest error values for the  $\chi^2$  (Chi-square), SE (Standard Error), and RMSE (Root Mean Square Error) functions with regards to the other models (Table 4), indicating that it was the best-fitting model, followed by the pseudo-second order (PSO) kinetic model. The vital concept that PSO fits

experimental data, according to Riahi *et al.* (2017), is that the rate-determining step is chemical reaction (chemisorption), which involves bond creation via electron exchange or sharing. Riahi and coworkers went on to say that Elovich's agreement with experimental data indicates that there are some heterogeneous surface adsorption, as well as a type of concurrent occurrence of intra-particle diffusion, precipitation, chemisorptions, and ion exchange with no way of knowing which one is dominant. The results of fitting Elovich and PSO to experimental data not only confirm chemisorption as the mechanism of reaction, but the two models also provide information on the quantity of dyes adsorbed per time (i.e. rate of adsorption) via their respective model parameters  $\alpha$  (mg/g/min) and  $K_1$  (g/mg/min), as shown in Table 4

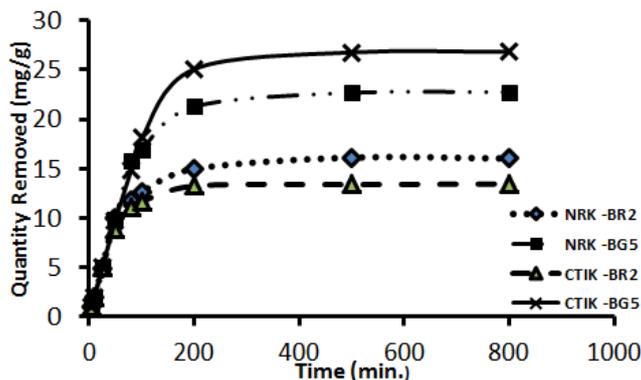


Figure 6: Effect of contact time on BR2 and BG5 uptake by NRK and CTIK

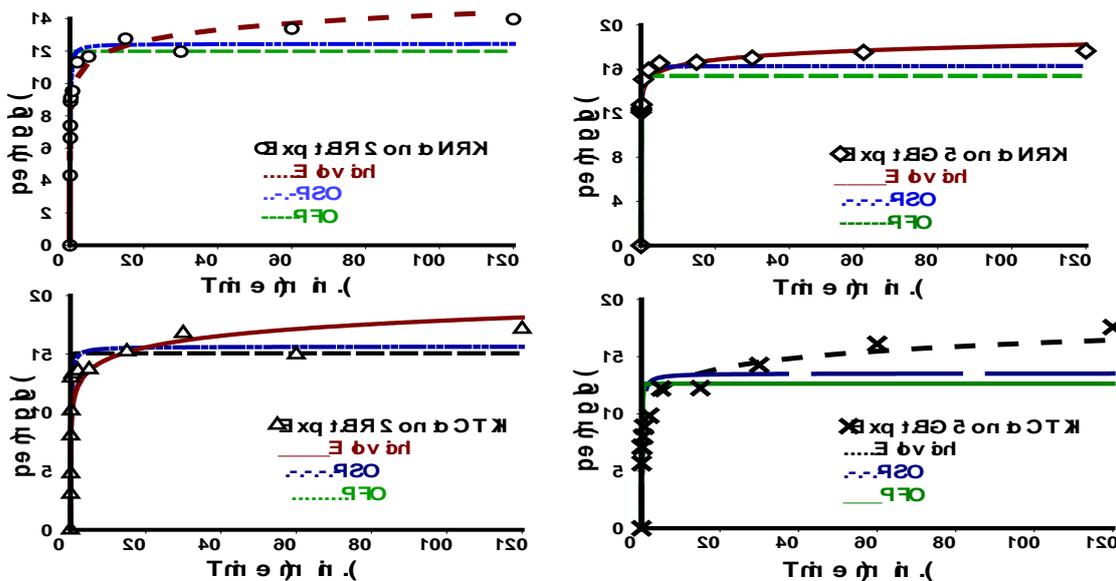


Figure 7: Non linear graphs for the fitting of the kinetic models

**Table 4 : Kinetic parameters for BR2 and BG5 dye molecules adsorption**

Kinetic	NRK		CTIK	
	BR2	BG5	BR2	BG5
<b>Pseudo-First Order</b>				
qe(mg/g)	12.42	12.45	14.25	13.99
K <sub>1</sub> (min <sup>-1</sup> )	3.90	4.23	9.50	3.77
R <sup>2</sup>	0.90	0.93	0.98	0.82
χ <sup>2</sup>	1.29	0.97	0.22	2.85
SE	1.43	1.26	0.67	2.38
RMSE	1.34	2.41	0.82	1.50
<b>Pseudo-Second Order</b>				
qe(mg/g)	0.49	0.54	1.97	0.37
K <sub>2</sub> (g/mg/mni)	12.89	12.89	14.45	14.59
R <sup>2</sup>	0.96	0.97	0.99	0.84
χ <sup>2</sup>	0.63	0.44	0.21	2.60
SE	0.96	0.83	0.53	2.23
RMSE	0.87	1.67	0.69	1.10
<b>Elovich</b>				
α(mg/g/min.)	1.18	1.25	1.57	0.83
β(g/mg) x10 <sup>6</sup>	0.14	0.31	341.69	0.01
R <sup>2</sup>	0.99	0.99	0.99	0.91
χ <sup>2</sup>	0.14	0.05	0.14	1.80
SE	0.45	0.28	0.62	1.67
RMSE	0.86	0.45	0.28	0.41

### Thermodynamic study

Thermodynamic parameters were studied in adsorption processes to investigate the effect of temperature on adsorbent – adsorbate interaction. The experimental process for the uptake of BR2 and BG5 basic dyes onto NRK and CTIK were carried out at three different temperatures (308, 313 and 318K). The adsorption capacities of both adsorbent increased steadily with temperature rise from 30 to 45°C. This observation confirms that there was an increase in the potential of the dye molecules ability to move across the adsorbent surface with increased temperature, resulting in an increase in adsorption capability.

Table 5 shows the values of the thermodynamic parameters. The values of  $\Delta G^\circ$  are negative for all the temperature of operation which an indication of spontaneous adsorption reaction. It is observable also as shown in Table 5, with increase in temperature there is a decrease in spontaneity of reaction an indication of endothermic reaction at high temperature. The negative value  $\Delta H^\circ$  confirms the adsorption process is exothermic nature. The entropy change has positive values ( $\Delta S^\circ$ ) meaning that there was an increase in disorderliness at the system's boundary interphase between the adsorbent and the adsorbate.

**Table 5: Thermodynamic quantities for BR2 and BG5 dyes adsorption**

Adsorbents	Adsorbate	$\Delta G^\circ \times 10^2$ (kJ/mol)			$\Delta H^\circ$ (kJ/mol)	$\Delta S^\circ \times 10^2$ (J/(mol.K))
		308 K	313 K	318K		
NRK	BR2	-21.76	-18.41	-0.71	-25.70	82.13
	BG5	-36.55	-23.08	-12.48	-29.64	95.71
CTIK	BR2	-17.89	-10.43	80.86	-120.37	374.60
	BG5	-26.90	-4.02	54.67	-99.87	311.60

### CONCLUSION

The efficiency of prepared CTAB – intercalated native raw kaolinite (CTIK) to remove Basic dyes from water was compared with that of native raw kaolinite adsorbent. The existence of extra functional atomic species on the surface of the CTIK adsorbent and the increase of the NRK interlayer space are indicators of successful adsorbent modification. The adsorption equilibrium was monomolecular on the surfaces of both

adsorbents, as predicted by the Sips isotherm model. Sips adsorption capacities for BR2 and BG5 dyes on NRK were 15.69 and 21.79 mg/g, respectively, and increased to 17.09 and 31.97 mg/g when adsorbed onto CTIK. The adsorption capability of these basic dyes is shown to be dependent on surface alkalinity. The kinetic study revealed that the adsorption of the BR2 and BG5 dyes follows the Elovich model, which is followed by pseudo-second-order kinetics, signifying an

irreversible reaction process and chemisorptions respectively. The thermodynamic parameter suggested that the adsorbent-adsorbate interaction was by exothermic process and practically spontaneous when the temperature of the system was increased.

**ACKNOWLEDGEMENTS:** We wish to thank the managements of University of Ibadan, Ibadan, Oyo State and Bells University of Technology, Ota, Ogun State, Nigeria for granting us permission to use their research laboratories. We are grateful.

**CONFLICT OF INTEREST:** The authors hereby declare that they have no conflict of interest

## REFERENCES

- Adebowale, K. O., Olu-Owolabi, B. I. and Chigbundu, C. E. (2014): Removal of Safranin-O from Aqueous Solution by Adsorption onto Kaolinite Clay. *Journal of Encapsulation and Adsorption Sciences* 4(3):89-104 DOI:10.4236/jeas.2014.43010
- Adegoke, H. I., Adekola, F. A. and Abdurraheem, M. N. (2017): Kinetic and Thermodynamic Studies on Adsorption of Sulphate from Aqueous Solution by Magnetite, Activated carbon and Magnetite-Activated Carbon Composites. *Nigerian Journal of Chemical Research*. 22 (1): 1-12.
- Adeyemo A.A., Adeoye I.O., and Bello O.S. (2017): Adsorption of dyes using different types of clay: a review, *Applied Water Science*. 7: 543–568.
- Adeyi, A., Abayomi, T., Purkait, M. and Mondal, P. (2019): Adsorptive Removal of Phosphate from Aqueous Solution by Magnetic-Supported Kaolinite: Characteristics, Isotherm and Kinetic Studies. *Open Journal of Applied Sciences*, 9: 544-563. doi: 10.4236/ojapps.2019.97043.
- Akyuz, S., Akyuz, T. and Davies, J.E.D. (1993): A vibrational spectroscopic study of the adsorption of 4,4'-bipyridyl by sepiolite and smectite group clay minerals from Anatolia (Turkey). *Journal of Inclusion Phenomena and Macrocyclic Chemistry*, 15:105–119
- Anirudhan T.S. and Ramachandran M. (2015): Adsorptive removal of basic dyes from aqueous solutions by surfactant modified bentonite clay (organoclay): kinetic and competitive adsorption isotherm. *Process Safety and Environmental Protection*, 95 : 215–225.
- Appel, C., Ma L. Q., Rhue R. D. and Kennelley E. (2003): Point of Zero Charge Determination in Soils and Minerals via Traditional Methods and Detection of Electroacoustic Mobility. *Geoderma* 113 (1 – 2) : 77-93. DOI:10.1016/S0016-7061(02)00316-6
- Aquino J. M., Rocha-Filho R.C., Ruotolo L. A., Bocchi N. and Biaggio S. R. (2014) Electrochemical degradation of a real textile wastewater using  $\beta$ -PbO<sub>2</sub> and DSA anodes. *Chemical Engineering Journal*, 251 : 138-145
- Ashtekar V. S., Bhandari V. M., Shirsath S. R., Sai Chandra P. L. V. N., Jolhe P. D. and Ghodke S. A. (2013): Dye wastewater treatment: removal of reactive dyes using inorganic and organic coagulants. *Journal of Industrial Pollution Control*, 30: 23 – 34
- Asuha, S., Gao, Z., Li, X., Wu, H., Zhao, S.M. and Deligeer, W. (2015): Magnetic Modification of Acid-Activated Kaolin: Synthesis, Characterization, and Adsorptive Properties. *Microporous and Mesoporous Materials*, 202: 1-7. <https://doi.org/10.1016/j.micromeso.2014.09.029>
- Austin, J. C., Perry, A., Richter, D. D. and Schroeder P. A. (2018): Modifications of 2:1 Clay Minerals in a Kaolinite-Dominated Ultisol under Changing Land-Use Regimes. *Clays and Clay Minerals*. 66: 61–73. <https://doi.org/10.1346/CCMN.2017.064085>
- Bakhtiary, S., Shirvani, M. and Shariatmadari, H. (2013): Characterization and 2,4-D Adsorption of Sepiolite Nanofibers Modified by N-Cetylpyridinium Cations. *Microporous and Mesoporous Materials*, 168 : 30-36. <https://doi.org/10.1016/j.micromeso.2012.09.022>
- Bennani-Karim A. Mounir B. Hachkar M. Bakasse M. and Yaacoubi A. (2011): Adsorption of malachite green dye onto raw Moroccan clay in batch and dynamic system. *Canadian Journal of environment and construction* 2:5–13
- Blistan, P., Jacko, S., Kovanič, E., Kondela, J., Pukanská, K., and Bartoš, K. (2020): TLS and SfM Approach for Bulk Density Determination of Excavated Heterogeneous Raw Materials. *Minerals*, 10 (2): 174. <https://doi.org/10.3390/min10020174>

- Boparai, H.K., Joseph, M. and O'Carroll, D.M. (2011): Kinetics and thermodynamics of cadmium ion removal by adsorption onto nanozerovalent iron particles. *Journal of Hazardous Material* 186:458–465. <https://doi.org/10.1016/j.jhazmat.2010.11.029>
- Boukhemkhem A. and Rida K. (2017): Improvement adsorption capacity of methylene blue onto modified Tamazert kaolin. *Adsorption Science and Technology* 35 . 9-10 : 753-773. doi:[10.1177/0263617416684835](https://doi.org/10.1177/0263617416684835)
- Lellis B., Fávaro-Polonio C. Z., Pamphile J. A and Polonio J. C. (2019): Effects of textile dyes on health and the environment and bioremediation potential of living organisms. *Biotechnology Research and Innovation*, 3(2):275-290, ISSN 2452-0721, <https://doi.org/10.1016/j.biori.2019.09.001>.
- Chaari I., Moussi B. and Jamoussi F. (2015): Interactions of the dye, C.I. direct orange 34 with natural clay. *Journal of Alloys and Compounds* 647 : 720–727.
- Charles L. Perrin (2019): Linear or Nonlinear Least-Squares Analysis of Kinetic Data?. *Journal of Chemical Education* 94 (6) : 669-672 DOI: 10.1021/acs.jchemed.6b00629
- Chigbundu C. E. and Adebawale K. O. (2021): Equilibrium and Kinetics Studies of the Adsorption of Basic Dyes onto PVOH Facilely Intercalated Kaolinite - A Comparative Study of Adsorption Efficiency. *Communication in physical sciences* 7 (4): 290 – 306.
- Aldhayan D. and Aouissi A. (2017): Gas Phase Oligomerization of Isobutene over Acid Treated Kaolinite Clay Catalyst. *Bulletin of Chemical Reaction Engineering and Catalysis* 12 (1) : 119-126
- Han H., Rafiq M.K., Zhou T., Xu R., Mašek O. and Li X. (2019): A critical review of clay-based composites with enhanced adsorption performance for metal and organic pollutants. *Journal of Hazardous Materials*.369: 780 – 790
- Hassan M.M. and Carr C.M. (2018): A critical review on recent advancements of the removal of reactive dyes from dyehouse effluent by ion-exchange adsorbents. *Chemosphere*, 209 (1): 201-219.
- Ibrahim, R. K., El-Shafie, A., Hin, L. S., Mohd, N. S. B., Aljumaily, M. M., Ibrahim, S., and AlSaadi, M. A. (2019): A clean approach for functionalized carbon nanotubes by deep eutectic solvents and their performance in the adsorption of methyl orange from aqueous solution. *Journal of environmental management*, 235, 521-534.
- Imran, M., Crowley, D. E., Khalid, A., Hussain S., Mumtaz M.W. and Arshad M. (2015): Microbial biotechnology for decolorization of textile wastewaters. *Reviews in Environmental Science and Biotechnology*, 14 (1): 73-92.
- Isiuku B.O., Iwu J.C., Emeagwara, D. C. and Ibe F.C. (2019): Adsorption performance of acid-activated carbon derived from *gmelina arborea* in batch removal of methyl violet from aqueous solution. *Journal of chemical society of Nigeria*,. 44 (1): 011 -021.
- Jadhav A. and Jadhav N. C. (2021): Treatment of textile wastewater using adsorption and adsorbents In book: *Sustainable Technologies for Textile Wastewater Treatments*. DOI: 10.1016/B978-0-323-85829-8.00008-0
- Khatri J., Nidheesh P.V., Singh T.A. and Kumar M.S. (2018): Advanced oxidation processes based on zero-valent aluminium for treating textile wastewater. *Chemical Engineering Journal*, 348 : 67-73
- Kodama, H. and Grim, R. E. (2014): clay mineral. Encyclopedia Britannica. <https://www.britannica.com/science/clay-mineral>.
- Kushwaha J. P. (2015): A review on sugar industry wastewater: sources, treatment technologies, and reuse. *Desalination and Water Treatment*.53 : 309-318.
- López-Luna, J. Ramírez Montes L. E., Vargas, SM. Martínez, O F. Ricardez, M. María del Carmen A. Chávez, G. González, R.C. Domínguez, FAS. Maríadel Carmen Cuevas Díaz and Virgilio Vázquez Hipólito (2019): Linear and nonlinear kinetic and isotherm adsorption models for arsenic removal by manganese ferrite nanoparticles. *SN Applied Sciences*, 1:950 <https://doi.org/10.1007/s42452-019-0977-3>
- Macías-Quiroga I. F., Giraldo-Gómez, G. I., and Sanabria-González, N. R. (2018): Characterization of Colombian Clay and Its Potential Use as Adsorbent. *The Scientific World Journal* 5969178. <https://doi.org/10.1155/2018/5969178>
- Maged A., Ismael I. S., Kharbish S., Sarkar B., Peräniemi S. and Bhatnagar A. (2020): Enhanced interlayer trapping of Pb(II) ions within kaolinite layers: intercalation, characterization, and sorption studies. *Environmental Science and Pollution Research* 27: 1870–1887. <https://doi.org/10.1007/s11356-019-06845-w>.

- Mahmood T., Saddique M. T., Naeem A., Westerhoff, P., Mustafa S. and Alum A. (2011): Comparison of different methods for the point of zero charge determination of NiO. *Industrial and Engineering Chemistry Research*. 50(17):10017–10023
- Martín, J., del Mar Orta, M., Medina-Carrasco, S., Santos, J. L., Aparicio, I., and Alonso, E. (2018): Removal of priority and emerging pollutants from aqueous media by adsorption onto synthetic organofunctionalized high-charge swelling micas. *Environmental research*, 164: 488-494.
- Mbaye A., Diop C. A. K., Jocelyne M. B. and François S. and Francis M. (2014): Characterization of natural and chemically modified kaolinite from Mako (Senegal) to remove lead from aqueous solutions. *Clay Minerals*, 49 .4 : 527-539. ISSN 0009-8558 .
- Meziane O., Bensedira A., Guessoum M. and Haddaoui N. (2017): Preparation and Characterization of Intercalated Kaolinite with: Urea, Dimethyl formamide and an Alkylammonium Salt Using Guest Displacement Reaction. *Journal of Materials and Environmental Sciences*. JMES. 8 .10: 3625-3635.
- Mincke S., Asere T. G., Verheye I., Folens K., Vanden B. F., Lapeire L., Verbeken K., Van Der Voort P., Tessema D. A., Fufa F., Du Laing, G. and Stevens C.V. (2019): Functionalized chitosan adsorbents allow recovery of palladium and platinum from acidic aqueous solutions. *The Royal Society of Chemistry* 1463-9262. <http://dx.doi.org/10.1039/C9GC00166B>
- Moussout, H. Ahlafi, H. Aazza, M. and Maghat H. (2018): Critical of linear and nonlinear equations of pseudo-first order and pseudo-second order kinetic models. *Karala International Journal of Modern Science*. 4 (2): 244-254
- Munir M., Ahmad M., Saeed M., Waseem A., Rehan M., Nizami A.-S., Zafar M., Arshad, M. and Sultana S. (2019): Sustainable production of bioenergy from novel non-edible seed oil (*Prunus cerasoides*) using bimetallic impregnated montmorillonite clay catalyst. *Renewable and Sustainable Energy Reviews*, 109 : 321.
- Mustapha S., Ndamitso M.M., Abdulkareem A.S., Tijani J.O., Mohammed A.K. and Shuaib D.T. (2019): Potential of using kaolin as a natural adsorbent for the removal of pollutants from tannery wastewater. *Heliyon*, 5 (11): 1 - 2, <https://doi.org/10.1016/j.heliyon.2019.e02923>.
- Nafees M. and Waseem A., (2014) Organoclays as Sorbent Material for Phenolic Compounds: A Review. *CLEAN* 42, 1500, 2014
- Nwosu F. O., Ajala O. J., Owoyemi R. M. and Raheem B. G. (2018): Preparation and characterization of adsorbents derived from bentonite and kaolin clays. *Applied Water Science*. 8:195 – 205, <https://doi.org/10.1007/s13201-018-0827-2>
- Obayomi, K. S. Auta, M. and Kovo, A. (2020): Isotherm, kinetic and thermodynamic studies for adsorption of lead(II) onto modified Aloji clay. *Desalination and Water Treatment*. 181: 376-384 DOI [10.5004/dwt.2020.25142](https://doi.org/10.5004/dwt.2020.25142)
- Omole, D. O., and Isiorho, S. (2011): Waste management and water quality issues in coastal states of Nigeria: The Ogun state experience. *Journal of Sustainable Development in Africa* , 13(6): 207–217.
- Overah L. C. (2020): Nonlinear Kinetic and Equilibrium Adsorption Isotherm Study of Cadmium (II) Sorption by *Dacryodes edulis* Biomass. *Nigerian Journal of Basic and Applied Science*, 28(2): 10-19 DOI: <http://dx.doi.org/10.4314/njbas.v28i2.2>
- Padmavathy K. S., Madhu G., Haseena. P.V. (2016): A study on effects of pH, adsorbent dosage, time, initial concentration and adsorption isotherm study for the removal of hexavalent chromium (Cr (VI)) from wastewater by magnetite nanoparticles. *Procedia Technology*, 24 : 585 – 594.
- Pei-Yee, A. Y., & Zaini, M. A. A. (2020): Decolourisation of malachite green dye by potassium carbonate-treated kernel shell adsorbent. *International Journal of Environment and Waste Management*, 25(4): 498-507.
- Perelomov, L. Mandzhieva, S. Minkina, T. Atroshchenko, Y., Perelomova, I., Bauer, T., Pinsky, D. and Barakhov, A. (2021). The Synthesis of Organoclays Based on Clay Minerals with Different Structural Expansion Capacities. *Minerals*, 11: 707. <https://doi.org/10.3390/min11070707>
- Rahmat U., Faiza J., I., Muhammad A., Afzal S, Mohammad S A., Haseeb U. and Amir W. (2020): Modified clays as an efficient adsorbent for brilliant green, ethyl violet and allura red dyes: Kinetic and thermodynamic studies. *Polish Journal of Environmental Studies*, 29 (5) 3831-3839. DOI: 10.15244/pjoes/112363.
- Rápó, E., and Tonk, S. (2021): Factors Affecting Synthetic Dye Adsorption; Desorption Studies: A Review of Results from the Last Five Years (2017-2021). *Molecules (Basel, Switzerland)*, 26 (17): 5419.

- <https://doi.org/10.3390/molecules26175419>
- Rashed MN. (2011): Acid Dye Removal from Industrial Wastewater by Adsorption on Treated Sewage Sludge. *International Journal of Environment and Waste Management* 7: 175-191.
- Riahi K., Chaabane S. and Thayer B. B. (2017): A kinetic modeling study of phosphate adsorption onto Phoenix dactylifera L. date palm fibers in batch mode. *Journal of Saudi Chemical Society*, 21 (1):143-152. <https://doi.org/10.1016/j.jscs.2013.11.007>
- Saikia B. J. and Parthasarathy G. (2010): Fourier Transform Infrared Spectroscopic Characterization of Kaolinite from Assam and Meghalaya, Northeastern India. *Journal of Modern Physics* 1: 206-210. Doi:10.4236/jmp.2010.14031
- Skripkina, T., Podgorbunskikh, E., Bychkov, A., and Lomovsky, O. (2020): Sorption of Methylene Blue for Studying the Specific Surface Properties of Biomass Carbohydrates. *Coatings*, 10(11): 1115.
- Šljivić-Ivanović, M. and Smičiklas, I (2020): 23 - Utilization of C&D waste in radioactive waste treatment—Current knowledge and perspectives, Editor(s): Fernando Pacheco-Torgal, Yining Ding, Francesco Colangelo, Rabin Tuladhar, Alexander Koutamanis, In Woodhead Publishing Series in Civil and Structural Engineering. *Advances in Construction and Demolition Waste Recycling*, Woodhead Publishing. Pages 475-500, <https://doi.org/10.1016/B978-0-12-819055-5.00023-1>.
- Sun K., Shi Y., Chen H., Wang X. and Li Z. (2017): Extending surfactant-modified 2:1 clay minerals for the uptake and removal of diclofenac from water. *Journal of Hazardous Material* 323A : 567-574
- Valdivia A. E. O., Osornio C. O., Vargas-Rodríguez Y. M. (2021): PBL with the Application of Multiple and Nonlinear Linear Regression in Chemical Kinetics and Catalysis. *American Journal of Educational Research*, 9 (1) 31-37 DOI:10.12691/education-9-1-4
- Vdović N., Jurina I., Škapin S. D. and Sondi I. (2010). The surface properties of clay minerals modified by intensive dry milling — revisited. *Applied Clay Science* 48 (4) : 575-580. <https://doi.org/10.1016/j.clay.2010.03.006>
- Yaseen D.A, and Scholz M. (2016): Shallow pond systems planted with Lemna minor treating azo dyes. *Ecological Engineering*, 94:295–305
- Yaseen, D.A., Scholz, M. (2019): Textile dye wastewater characteristics and constituents of synthetic effluents: a critical review. *Int. J. Environ. Sci. Technol.* 16: 1193–1226. <https://doi.org/10.1007/s13762-018-2130-z>
- Yousefi, N., Wong, K. K., Hosseinidoust, Z., Sørensen, H. O., Bruns, S., Zheng, Y., and Tufenkji, N. (2018): Hierarchically porous, ultra-strong reduced graphene oxide-cellulose nanocrystal sponges for exceptional adsorption of water contaminants. *Nanoscale*, 10 (15): 7171-7184.
- Zakaria, M, Bains R. and Zauzi, N. (2017): Effect of pH, Dosage and Concentration on the Adsorption of Congo Red onto Untreated and Treated Aluminium Dross. *Materials Science and Engineering* 205 (1):012026 DOI: 10.1088/1757-899X/205/1/012026
- Zenasni M., Meroufel, B., Merlin, A. and George, B. (2014): Adsorption of Congo Red from Aqueous Solution Using CTAB-Kaolin from Bechar Algeria. *Journal of Surface Engineered Materials and Advanced Technology* 4 : 332-341. doi: [10.4236/jsemat.2014.46037](https://doi.org/10.4236/jsemat.2014.46037).
- Zuo X., Wang D., Zhang S., Liu Q. and Yang H. (2017). Effect of Intercalation Agents on Morphology of Exfoliated Kaolinite. *Minerals* 7: 249 - 261; doi:10.3390/min7120249



## Levels of Heavy Metals in Lipsticks Commonly and Commercially Available in Benin City, Nigeria

**\*Jacob, J. N. and Ebhota, M. I.**

Department of Chemistry, Faculty of Physical Sciences, University of Benin, Benin City, Edo State, Nigeria

**\*Correspondence Email:** jacob.jacob@uniben.edu

### ABSTRACT

This research was carried-out to assess the levels of heavy metals (Hg, As, Cd, Sb and Pb) concentration in selected lipsticks commonly and commercially available in Benin city, Nigeria. Ten (10) different brands of lipstick (5 each) were randomly selected across the four (04) local government areas that made up Benin city. The samples were ground and mixed to form a composite sample of each brand, digested and analyzed using Atomic Absorption Spectrophotometer (AAS). The analyses were done in triplicates and the mean concentration of arsenic were determined to be in the range of 4.90 – 369.85µg/g, mercury in the range of range of 4.99 – 60.42µg/g, antimony 4.94 – 20.39µg/g, cadmium 8.44 – 95.50 µg/g, and lead in the range of 33.17 – 69.33 µg/g. The metals concentration obtained were found be above the permissible limits set by WHO and USFDA. The results showed that the continuous use of these lipsticks brands poses a risk to the health of the users. Hence, stringent measures needs to be adopted during manufacturing to avoid the presence of these toxic metals as impurities and also, government regulations needs to be put in place to monitor the quality of lipsticks imported into the country.

**Keywords:** Benin city, Heavy metals, Lipsticks, Nigeria

### INTRODUCTION

Cosmetics have been used right from the beginning of time. It is a personal care products used by all types of people all over the globe. According to the United States Food and Drug Administration (USFDA, 2018), “cosmetics are articles intended to be rubbed, poured, sprinkled or sprayed on, introduced into or otherwise applied to the human body or any part thereof for cleansing, beautifying, promoting attractiveness or altering the appearance”.

Lipsticks are one of the cosmetics that are widely used throughout the world, most especially by the female gender. Lipsticks contain oils, silica, emollients, mica, titanium dioxide, antioxidant materials and colourants which give distinct appearances and hues to the finished product (Ezeh *et al.*, 2019). Lipstick has variety of colours cause by the introduction of organic or inorganic pigments. Heavy metals have been reported to be present in most lipsticks (Adepoju-Bello *et al.*, 2012; Oklo *et al.*, 2020; Alam *et al.*, 2019; Ezeh *et al.*, 2019; Ayuba *et al.*, 2017) and this could be introduced as part of the ingredients or impurities. Adulteration of lipstick products with heavy metals takes place during the process of production or lack of adequate purification of basic materials used for production (Ezeh *et al.*, 2019). These heavy metals can be very harmful even at low concentration and a bioaccumulation of these metals can spell doom

to human health if not properly and routinely checked.

According to Sainio *et al.* (2000), the key toxic metals in cosmetics especially lipsticks are chromium, lead, antimony, arsenic, cadmium and mercury. Since lipsticks are applied on lips around the mouth, it is expected that oral exposure to these impurities present in lipsticks can occur which can lead to deterioration of health on prolong exposure. Due the report by many researchers of the availability of heavy metals in lipsticks used in many countries, the United States government in 2013 imposed limits for some metals in cosmetics; 3µg/g for As, Cd and Hg, 5µg/g for Sb, 170µg/g for Ni, Cr, Co and Cu, and 20µg/g for Pb (USFDA, 2013) while world health organization (WHO) has set 10 µg/g for Pb, 0.3 µg/g for Cd and 1 µg/g for Hg as permissible limits (WHO, 2010).

The application of cosmetics especially lipsticks by Bini women is a long aged custom and the use of this product (both locally and foreign made) by Bini women in recent times has increased in alarming rate. However, there is limited information on the level of heavy metals in lipsticks commonly found in Nigerian markets and Benin city in particular. Therefore there is need for continuous investigation and monitoring of the level of heavy metals in lipsticks commercially available in Benin city. Hence, this research is focused on the assessment of the concentration of heavy metals (mercury, lead, antimony, arsenic and